Journal of Zhejiang University SCIENCE A
ISSN 1673-565X (Print); ISSN 1862-1775 (Online)
www.zju.edu.cn/jzus; www.springerlink.com
E-mail: jzus@zju.edu.cn

Semi-analytical Monte Carlo simulation of laser-induced fluorescence propagation in an optically participating spray*

CHEN Ling-hong†1, ROZE Claude[2], GARO Annie[2], GIRASOLE Thierry[2], CEN Ke-fa[1], GREHAN Gérard[2]

([1]*State Key Laboratory of Clean Energy Utilization, Zhejiang University, Hangzhou 310027, China*)

([2]*Laboratoire d'Electromagnétisme et Systèmes Particulaires, Universite & INSA Rouen, CORIA/CNRS UMR 6614, France*)

†E-mail: chenlh@zju.edu.cn

Received Dec. 19, 2006; revision accepted Mar. 28, 2007

Abstract: A semi-analytical Monte Carlo (SMC) simulation was developed to simulate the propagation of laser-induced fluorescence (LIF) in an optically participating spray, which simultaneously exhibits spectrally dependent emission, anisotropic scattering, absorption, and re-emission. The SMC simulation is described and then applied to an experimental configuration of a cloud of polydisperse droplets composed of water and sulforhodamine B dye. In the SMC simulation, the collected LIF flux on the remote receptor element is calculated as the global contribution from the emissive source, single, twice, … and *n*th collision events in any sequence. The effects on the fluorescence photons propagation of spray parameters like the dye concentration, droplets concentration, and droplets size are examined. Three spectral bands representing different optical properties are chosen to analyze the interference of absorption, scattering and re-emission on the detected LIF flux. The obtained spectral LIF flux distribution on the receptor demonstrates a "red shift" phenomenon.

Key words: Laser-induced fluorescence (LIF), Semi-analytical Monte Carlo (SMC) simulation, Absorption, Anisotropic scattering, Re-emission, Spray

doi:10.1631/jzus.2007.A1170 **Document code:** A **CLC number:** O21; O43; TK01

INTRODUCTION

Recently, laser-induced fluorescence (LIF) techniques have been widely used to study species concentration, pressure, temperature and velocity in flames and droplet sprays (Castanet *et al.*, 2002; Lavieille *et al.*, 2001; 2004; Lemoine *et al.*, 1999). In many optical diagnostics, the LIF technique permits the determination of the sample's structure and components in a non-intrusive way without leaving a degree of uncertainty due to the sampling process and through transport of the particles samples to the device (Chen *et al.*, 1996). The use of the LIF techniques is preferred when the samples are transparent.

The existence of scattering, absorption and re-emission from the particles sample may degrade the performance of the LIF techniques by (1) reducing the number of the excitation photons that reach the focal volume of the particles sample; (2) decreasing the number of fluorescence photons that can reach the small area receiver; (3) introducing fluorescence photons from nonconjugate regions in the sample. The above factors result in the loss of fluorescence signal details and contrast degradation for the generated fluorescence signal.

The accurate prediction of the fluorescence propagation within the participating media becomes a formidable task when the spectral anisotropic scattering, absorption and re-emission characteristics of the sample are considered. These characteristics are difficult to investigate experimentally. Numerical simulations can be stochastic (Rozé *et al.*, 2003). Some researchers used MC simulation to analyze fluorescence propagation in scattering sample (Blanca and Saloma, 1998; Wang *et al.*, 1995). MC simulation

* Project supported by the National Natural Science Foundation of China (No. 60534030), and the Scholarship of French Embassy in China and the Doctoral Grant from French Embassy in China

has also been used to investigate the absorption and fluorescence spectra of a model diatomic solute in a methyl iodide solvent (Gomez and Thompson, 2004). To our best knowledge, no research has been reported so far on the prediction of LIF propagation when the particles sample simultaneously exhibits spectral emission, anisotropic scattering, absorption, and re-emission behaviors.

In this research, an improved MC method called "semi-analytical Monte Carlo" (SMC) method was developed to predict LIF propagation within an optically participating spray which simultaneously exhibits spectral emission, anisotropic scattering, absorption and re-emission behaviors. The developed SMC method considers the independent scattering (Brewster and Tien, 1982) and re-emission problems by neglecting the effects of the diffraction and interference between the various scattered and re-emitted excitation waves and internal fields.

An experimental set-up consisting of LIF droplets within a cylindrical optically participating spray has been chosen as a test configuration for the SMC simulation. The detected LIF flux on the remote receptor element was investigated. The influences of spray parameters on the detected LIF fluxes sensitivity are calculated, and a red-shift phenomenon of the spectral detected LIF flux is distinguished.

FLUORESCENCE SIMULATION MODEL

Analysis of LIF propagation in an optically participating spray

The test configuration set-up for the SMC simulation is a simplified scheme of a laboratory experiment realized by a research team in France (Lavieille *et al*., 2001). The spray is assumed cylindrical with a spray diameter D_c and a height H_c, shown on Fig.1. The liquid spray is composed of a cloud of polydisperse spherical droplets. The excitation laser beam is focused inside the spray. The control volume on the focused location is assumed to be small enough to contain a unique droplet located at the center of the spray. The droplet is considered as the LIF emission source in the SMC simulation. A receptor with a section element is located outside the spray at the distance of X_c. The air interference is neglected.

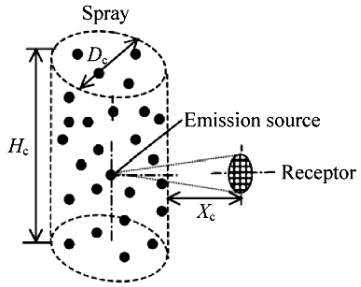

Fig.1 The schematic test configuration for the SMC simulation

For the LIF emission within the cylindrical spray, the spectral LIF flux on the receptor area can be considered as the global contribution from the emissive source, 1st, 2nd, …, *n*th collision events:

$$\mathrm{d}\Phi_\lambda=\mathrm{d}\Phi_{\mathrm{emit},\lambda}+\mathrm{d}\Phi_{\mathrm{sca},\lambda}+\mathrm{d}\Phi_{\mathrm{re\text{-}emit},\lambda}. \quad (1)$$

The first term on the right of the equation represents the detected flux from the emissive droplet source, the second term refers to the sum of fluxes generated by single, twice, …, *n*th scattering events, and the last term refers to absorption and re-emitted events.

1. The detected flux from the emissive source location

The spectral fluorescent flux from the source point impinging directly on the receptor within an infinitesimal solid angle $\mathrm{d}\boldsymbol{\Omega}_s$ and a wavelength interval $\mathrm{d}\lambda_s$, seen on Fig.2, can be calculated by:

$$\mathrm{d}\Phi_{\mathrm{emit},\lambda_s}=\int_{\boldsymbol{x}_s\in S} I_{\lambda_s}(\boldsymbol{x}_0,\boldsymbol{\Omega}_s)\exp(-k_{\mathrm{ext},\lambda_s}x_s)\mathrm{d}\boldsymbol{\Omega}_s\mathrm{d}\lambda_s, \quad (2)$$

where $\boldsymbol{x}_0$ represents the location of emissive source, and $\boldsymbol{x}_s$ the location of receptor. λ_s is the detected wavelength. $\boldsymbol{\Omega}_s$ is the direction from the emissive source $\boldsymbol{x}_0$ to the receptor element $\boldsymbol{x}_s$. $I_{\lambda_s}(\boldsymbol{x}_0,\boldsymbol{\Omega}_s)$ is the

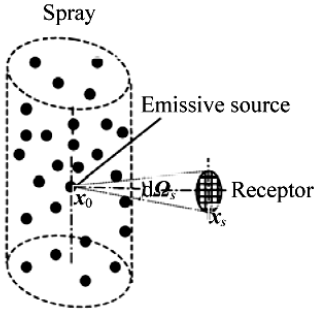

Fig.2 The detected LIF flux from the emissive source point

spectral fluorescent intensity at the emissive source. $k_{\mathrm{ext},\lambda_s}$ is the spectral extinction coefficient. The distance between the locations $\boldsymbol{x}_0$ and $\boldsymbol{x}_s$ is defined as $\|\boldsymbol{x}_s-\boldsymbol{x}_0\|$. Then the part of this distance within the spray x_s is equal to ($\|\boldsymbol{x}_s-\boldsymbol{x}_0\|-X_c$). $\mathrm{d}\boldsymbol{\Omega}_s$ is an elemental solid angle corresponding to a small surface around a point $\boldsymbol{x}_s$ on the receptor area S seen from the emissive source $\boldsymbol{x}_0$.

2. The detected fluxes generated by the single collision event

For each point referred by its vector-coordinates $\boldsymbol{x}_1$ within the spray, the flux arriving on the receptor area consists of "photons" scattered once and verifies:

$$\mathrm{d}\Phi^1_{\mathrm{sca},\lambda_s}=\int_{\boldsymbol{x}_s\in S}\int_{\boldsymbol{x}_1\in V}[I_{\lambda_s}(\boldsymbol{x}_0,\boldsymbol{\Omega}_1)\exp(-k_{\mathrm{ext},\lambda_s}x_1)\mathrm{d}\boldsymbol{\Omega}_1\mathrm{d}\lambda_s k_{\mathrm{sca},\lambda_s}\cdot\mathrm{d}\boldsymbol{x}_1 f(\boldsymbol{\Omega}_1,\boldsymbol{\Omega}_s)\mathrm{d}\boldsymbol{\Omega}_s\exp(-k_{\mathrm{ext},\lambda_s}x_s)], \quad (3)$$

where $\boldsymbol{\Omega}_1$ is the unit vector of the direction from the emissive location $\boldsymbol{x}_0$ to the scattered location $\boldsymbol{x}_1$. $\boldsymbol{\Omega}_s$ is the direction from the point $\boldsymbol{x}_1$ to the receptor element $\boldsymbol{x}_s$. $k_{\mathrm{sca},\lambda_s}$ is the spectral scattering coefficient at the wavelength λ_s. The scattering phase function $f(\boldsymbol{\Omega}_1,\boldsymbol{\Omega}_s)$ is the probability that a photon from the direction $\boldsymbol{\Omega}_1$ propagates toward the receptor area $\boldsymbol{\Omega}_s$. The distance x_1 is defined by $\|\boldsymbol{x}_1-\boldsymbol{x}_0\|$, and the distance x_s is the part of the path $\|\boldsymbol{x}_s-\boldsymbol{x}_1\|$ within the spray.

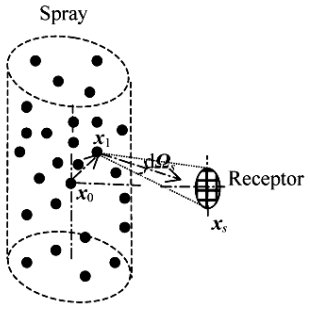

Fig.3 The detected flux from the first scattering or re-emitting event location

For the case of single re-emitting event, the amount of flux onto the receptor is:

$$\mathrm{d}\Phi^1_{\text{re-emit},\lambda_s}=\int_{\boldsymbol{x}_s\in S}\int_{\lambda_1<\lambda_s}\int_{\boldsymbol{x}_1\in V}[I_{\lambda_1}(\boldsymbol{x}_0,\boldsymbol{\Omega}_1)\exp(-k_{\mathrm{ext},\lambda_1}x_1)\cdot\mathrm{d}\boldsymbol{\Omega}_1\mathrm{d}\lambda_1 k_{\mathrm{abs},\lambda_1}\mathrm{d}\boldsymbol{x}_1 q\varepsilon_{\lambda_1,\lambda_s}\mathrm{d}\lambda_s f'(\boldsymbol{\Omega}_1,\boldsymbol{\Omega}_s)\mathrm{d}\boldsymbol{\Omega}_s\cdot\exp(-k_{\mathrm{ext},\lambda_s}x_s)], \quad (4)$$

where λ_1 is the wavelength before re-emitted. λ_s is the wavelength after re-emitted. $k_{\mathrm{abs},\lambda_1}$ is the spectral absorption coefficient. $k_{\mathrm{abs},\lambda_1}\mathrm{d}\boldsymbol{x}_1$ is the fraction of absorption along an infinitesimal $\mathrm{d}\boldsymbol{x}_1$. The quantum yield q is the probability absorbed and converted to fluorescence. $\varepsilon_{\lambda_1,\lambda_s}\mathrm{d}\lambda_s$ is the fraction of fluorescence re-emitted from λ_1 into λ_s. The part $q\varepsilon_{\lambda_1,\lambda_s}\mathrm{d}\lambda_s$ is the fraction absorbed and re-emitted into another infinitesimal wavelength interval $\mathrm{d}\lambda_s$ around λ_s. The re-emitted phase function $f'(\boldsymbol{\Omega}_1,\boldsymbol{\Omega}_s)$ describes the probability of being re-emitted into the direction $\boldsymbol{\Omega}_s$ from the direction $\boldsymbol{\Omega}_1$.

3. The detected fluxes from the second collision event

Before the second scattering event, there exist two kinds of cases for the first collision: one case is scattering, the other is absorption and re-emission. So the flux from the second collision event of scattering can be calculated by:

$$\begin{aligned}\mathrm{d}\Phi^2_{\mathrm{sca},\lambda_s}=&\int_{\boldsymbol{x}_s\in S}\int_{\boldsymbol{x}_2\in V}\int_{\boldsymbol{x}_1\in V}\{[I_{\lambda_s}(\boldsymbol{x}_0,\boldsymbol{\Omega}_1)\exp(-k_{\mathrm{ext},\lambda_s}x_1)\mathrm{d}\boldsymbol{\Omega}_1\\&\cdot\mathrm{d}\lambda_s k_{\mathrm{sca},\lambda_s}\mathrm{d}\boldsymbol{x}_1 f(\boldsymbol{\Omega}_1,\boldsymbol{\Omega}_2)\mathrm{d}\boldsymbol{\Omega}_2\exp(-k_{\mathrm{ext},\lambda_s}x_2)\\&\cdot k_{\mathrm{sca},\lambda_s}\mathrm{d}\boldsymbol{x}_2 f(\boldsymbol{\Omega}_2,\boldsymbol{\Omega}_s)\mathrm{d}\boldsymbol{\Omega}_s\exp(-k_{\mathrm{ext},\lambda_s}x_s)]\\&+\int_{\lambda_1<\lambda_s}[I_{\lambda_1}(\boldsymbol{x}_0,\boldsymbol{\Omega}_1)\exp(-k_{\mathrm{ext},\lambda_1}x_1)\mathrm{d}\boldsymbol{\Omega}_1\mathrm{d}\lambda_1 k_{\mathrm{abs},\lambda_1}\\&\cdot\mathrm{d}\boldsymbol{x}_1 q\varepsilon_{\lambda_1,\lambda_s}\mathrm{d}\lambda_s f'(\boldsymbol{\Omega}_1,\boldsymbol{\Omega}_2)\mathrm{d}\boldsymbol{\Omega}_2\exp(-k_{\mathrm{ext},\lambda_s}x_2)\\&\cdot k_{\mathrm{sca},\lambda_s}\mathrm{d}\boldsymbol{x}_2 f(\boldsymbol{\Omega}_2,\boldsymbol{\Omega}_s)\mathrm{d}\boldsymbol{\Omega}_s\exp(-k_{\mathrm{ext},\lambda_s}x_s)]\}. \quad (5)\end{aligned}$$

The amount of flux onto the receptor from the second collision event of absorption and re-emission is:

$$\begin{aligned}\mathrm{d}\Phi^2_{\text{re-emit},\lambda_s}=&\int_{\boldsymbol{x}_s\in S}\int_{\boldsymbol{x}_2\in V}\int_{\boldsymbol{x}_1\in V}\{\int_{\lambda_1<\lambda_s}[I_{\lambda_1}(\boldsymbol{x}_0,\boldsymbol{\Omega}_1)\mathrm{d}\boldsymbol{\Omega}_1\\&\cdot\exp(-k_{\mathrm{ext},\lambda_1}x_1)\mathrm{d}\lambda_1 k_{\mathrm{sca},\lambda_1}\mathrm{d}\boldsymbol{x}_1 f(\boldsymbol{\Omega}_1,\boldsymbol{\Omega}_2)\mathrm{d}\boldsymbol{\Omega}_2\\&\cdot\exp(-k_{\mathrm{ext},\lambda_1}x_2)k_{\mathrm{abs},\lambda_1}\mathrm{d}\boldsymbol{x}_2 q\varepsilon_{\lambda_1,\lambda_s}\mathrm{d}\lambda_s f'(\boldsymbol{\Omega}_2,\boldsymbol{\Omega}_s)\\&\cdot\mathrm{d}\boldsymbol{\Omega}_s\exp(-k_{\mathrm{ext},\lambda_s}x_s)]+\int_{\lambda_2<\lambda_s}\int_{\lambda_1<\lambda_2}[I_{\lambda_1}(\boldsymbol{x}_0,\boldsymbol{\Omega}_1)\\&\cdot f'(\boldsymbol{\Omega}_1,\boldsymbol{\Omega}_2)\mathrm{d}\boldsymbol{\Omega}_2\mathrm{d}\boldsymbol{\Omega}_1\exp(-k_{\mathrm{ext},\lambda_1}x_1)\mathrm{d}\lambda_1 k_{\mathrm{abs},\lambda_1}\mathrm{d}\boldsymbol{x}_1\\&\cdot q\varepsilon_{\lambda_1,\lambda_2}\mathrm{d}\lambda_2\exp(-k_{\mathrm{ext},\lambda_2}x_2)k_{\mathrm{abs},\lambda_2}\mathrm{d}\boldsymbol{x}_2 q\varepsilon_{\lambda_2,\lambda_s}\mathrm{d}\lambda_s\\&\cdot f'(\boldsymbol{\Omega}_2,\boldsymbol{\Omega}_s)\mathrm{d}\boldsymbol{\Omega}_s\exp(-k_{\mathrm{ext},\lambda_s}x_s)]\}. \quad (6)\end{aligned}$$

Before the nth collision events, there exists 2^{n-1} kind of cases for 1, 2, …, (n−1)th collision events of

scattering and re-emission. So Eq.(1) becomes an expression of multiple integrals with nth scattering and re-emission.

Description of SMC simulation

The SMC simulation is to solve the fluorescence propagation Eq.(1) composed of the following modules.

1. The photon tracing module

A large number of photons start from the LIF emissive resource, i.e. the droplet located in the focus volume within the spray. The studied fluorescence spectra are separated into several wavelength bands with each band being divided into small wavelength intervals. In each wavelength interval, the initial energy carried by each photon is driven by the ratio of the corresponding emitting band and of the whole band energy. Each "LIF photon" launching is assumed isotropic and its trajectory is described by the zenith angle θ and the azimuth angle φ:

$$\theta=\arccos(2R_1-1), \tag{7}$$

$$\varphi=2\pi R_2, \tag{8}$$

where R_1 and R_2 are equidistributed random numbers between 0 and 1.

2. The collision event

The extinction coefficient $k_{\text{ext},\lambda}$ is used to compute the collision distance l between the photon location and the first location of collision by a droplet.

$$l=-\ln R_3/k_{\text{ext},\lambda}, \tag{9}$$

where R_3 is an equidistributed random number between 0 and 1.

At each collision event, the comparison between albedo ($=k_{\text{sca},\lambda}/k_{\text{ext},\lambda}$) with an equidistributed random number is used to decide if the photon is absorbed or scattered.

After the scattering collision, the "scattered photon" carrying the same energy travels at the same incident wavelength along a new direction. This new direction is determined by the mean scattering phase function:

$$R_4=\int_0^{\boldsymbol{\Omega}} f(\boldsymbol{\Omega})\mathrm{d}\boldsymbol{\Omega}\Big/\int_0^{4\pi} f(\boldsymbol{\Omega})\mathrm{d}\boldsymbol{\Omega}, \tag{10}$$

where R_4 is an equidistributed random number between 0 and 1.

After an absorption followed by a new emission (i.e. "re-emission" event), the travelling direction followed by a re-emitted photon is assumed to be isotropic, and generated by an equidistributed random number between 0 and 1. At each absorption event, a complementary comparison between an equidistributed random number and the fluorescence quantum yield is used to decide if the absorption is followed by a "re-emission" or not. The re-emission wavelength is determined by:

$$R_5=\int_{\lambda_i}^{\lambda} k_{\text{emit},\lambda}\mathrm{d}\lambda\Big/\int_{\lambda_i}^{\lambda_{\max}} k_{\text{emit},\lambda}\mathrm{d}\lambda, \tag{11}$$

where R_5 is an equidistributed random number between 0 and 1. λ_i represents the current excitation wavelength at the re-emission collision. $k_{\text{emit},\lambda}$ is the coefficient of fluorescence emission.

3. The analytical module

In the case of the scattering collision, a small energy fraction that is nth scattered through the angle ($\boldsymbol{\Omega}_n$, $\boldsymbol{\Omega}_s$) toward the direction $\boldsymbol{\Omega}_s$, which lies within the small solid angle $\mathrm{d}\boldsymbol{\Omega}_s$ subtended by the receptor area from the nth scattered location to the receptor element. The scattering phase function $f(\boldsymbol{\Omega}_n, \boldsymbol{\Omega}_s)$, assumed as a constant over an element of solid angle $\mathrm{d}\boldsymbol{\Omega}_s$, gives the energy fraction of the photon coming from the direction $\boldsymbol{\Omega}_n$ and scattered into $\mathrm{d}\boldsymbol{\Omega}_s$ along the direction $\boldsymbol{\Omega}_s$. In the SMC approach, Eq.(12) gives the LIF flux collected by the remote receptor element after a scattering event at nth scattered location without any interaction within the spray:

$$q_\lambda=Wf(\boldsymbol{\Omega}_n,\boldsymbol{\Omega}_s)\exp(-k_{\text{ext},\lambda_s}x_n)\mathrm{d}\boldsymbol{\Omega}_s, \tag{12}$$

where W is a constant representing the droplet properties. x_n is the part distance within the spray along the nth scattered location to the receptor element.

An analogous relationship can be written for the absorption and re-emission event by introducing the re-emission phase function $f'(\boldsymbol{\Omega}_n, \boldsymbol{\Omega}_s)$, a function characterizing the angular emission pattern of the droplet.

RESULTS AND DISCUSSIONS

A cylindrical spray of $D_c \times H_c$ (=200 mm×500 mm) is composed of a cloud of polydisperse spherical droplets of water and a dye: sulforhodamine B ($C_{27}H_{30}N_2O_7S_2$). The excitation laser beam at a wavelength of 514.5 nm is focused inside the spray. The control volume on the focused location is assumed to be small enough to contain a unique droplet located at the center of the spray. The droplet is considered as the LIF emission source in the SMC simulation. A receptor element is located outside the spray at the distance of X_c=100 mm. The air interference is neglected.

The complex refractive index of sulforhodamine B in water was described in (Chen, 2005). The spectral cross sections and phase function are computed by Mie theory for a spherical droplet (Bohren and Huffman, 1983; Gouesbet and Gréhan, 2000). An assumed Gaussian size distribution of spherical droplets $\varphi(r)$ was introduced in the numerical simulation. The mean value of extinction, scattering coefficients and phase function are characterised by:

$$k_{\text{ext},\lambda} = \int_{r_{\min}}^{r_{\max}} C_{\text{ext},\lambda}(r)\varphi(r)\mathrm{d}r, \tag{13}$$

$$k_{\text{sca},\lambda} = \int_{r_{\min}}^{r_{\max}} C_{\text{sca},\lambda}(r)\varphi(r)\mathrm{d}r, \tag{14}$$

$$f_\lambda(\boldsymbol{\Omega}) = \frac{\int_{r_{\min}}^{r_{\max}} f_\lambda(r) C_{\text{ext},\lambda}(r)\varphi(r)\mathrm{d}r}{\int_{r_{\min}}^{r_{\max}} C_{\text{ext},\lambda}(r)\varphi(r)\mathrm{d}r}, \tag{15}$$

where the values of $r_{\min}$ and $r_{\max}$ represent the minimum and maximum of droplet size, respectively.

In this paper, the value of quantum yield for sulforhodamine B in water is supposed as unity (Chen, 2005).

Fig.4 gives the absorption and LIF emission spectra of sulforhodamine B in water with 5×10^{-6} mol/L at 20°C, the mean droplets radius is equal to 20 μm. We can find that the absorption and emission characteristics of dyed droplets are strongly dependent on the wavelength.

In the SMC simulations, the fluorescence flux on the receptor area (called as "global detected" flux) is obtained by adding all the partial fluxes from: the emissive source i.e. "direct" flux, absorption and re-emission events i.e. "re-emitted" flux, and scattering collisions. The single scattering event gives a "single scattered" flux, twice, and more than twice scattering events as "multiple scattered" flux. The simulation is performed for successive anisotropic scattering and re-emission events in any sequence.

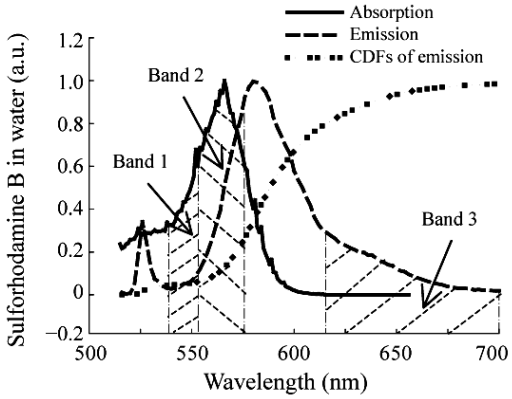

Fig.4 Input profiles: absorption and fluorescence spectra of sulforhodamine B in water with 5×10^{-6} mol/L at 20 °C, mean radius of droplets r=20 μm. 'CDFs of emission' means Cumulative Distribution Function of fluorescent emission spectra

Numerical simulation was made to investigate the effects of droplet concentration, dye concentration, and size of droplets on the detected fluorescence flux. The simulated cases refer successively to the dye concentrations: 3×10^{-7}, 3×10^{-6}, 3×10^{-5}, 3×10^{-4}, 3×10^{-3} mol/L, to the mean droplets diameters: 1, 5, 10, 50, 100 μm, and to the droplets concentrations: 10^8, 10^9, 10^{10}, 5×10^{10}, 10^{11} droplets/m^3.

The simulated results are discussed firstly about the partial detected fluxes in the three spectral bands standing for different optical properties: band 1 (the wavelengths between 535 nm and 555 nm) is chosen as the band where absorption but no emission occurs; band 2 (555 nm and 575 nm) with both absorption and emission; band 3 (615 nm and 700 nm) with emission but without absorption. Then the global spectral detected fluxes are investigated. The fluoresecent spectra between 515 nm and 700 nm are analyzed.

Partial fluxes in the three chosen spectral bands

1. The effects of the dye concentration

Fig.5a and Fig.5b give the partially detected LIF fluxes from the scattering events exclusively at the above three spectral bands. The single and multiple scattered fluxes at the spectral bands 1 and 2 are not sensitive to dye concentrations lower than 3×10^{-5}

mol/L. However, the scattered fluxes in spectral bands 1 and 2 decrease with dye concentration above 3×10^{-5} mol/L. This can be explained by the value of the cross sections of absorption and scattering, shown on Fig.6a and Fig.6b. At the moderate values of dye concentration, $C_{sca,\lambda}$ is much smaller than $C_{sca,\lambda}$, almost no photon absorption following a droplet collision can occur. Increasing the dye concentration generates an increase of the spectral absorption cross sections in the bands 1 and 2, whereas the scattering cross section $C_{sca,\lambda}$ decreases. Consequently, the probability of an energy absorption after a collision event increases with the dye concentration.

As seen in Fig.4, the band 2 corresponds to the strongest absorption, the scattering fluxes at band 2 decreases more quickly than at band 1.

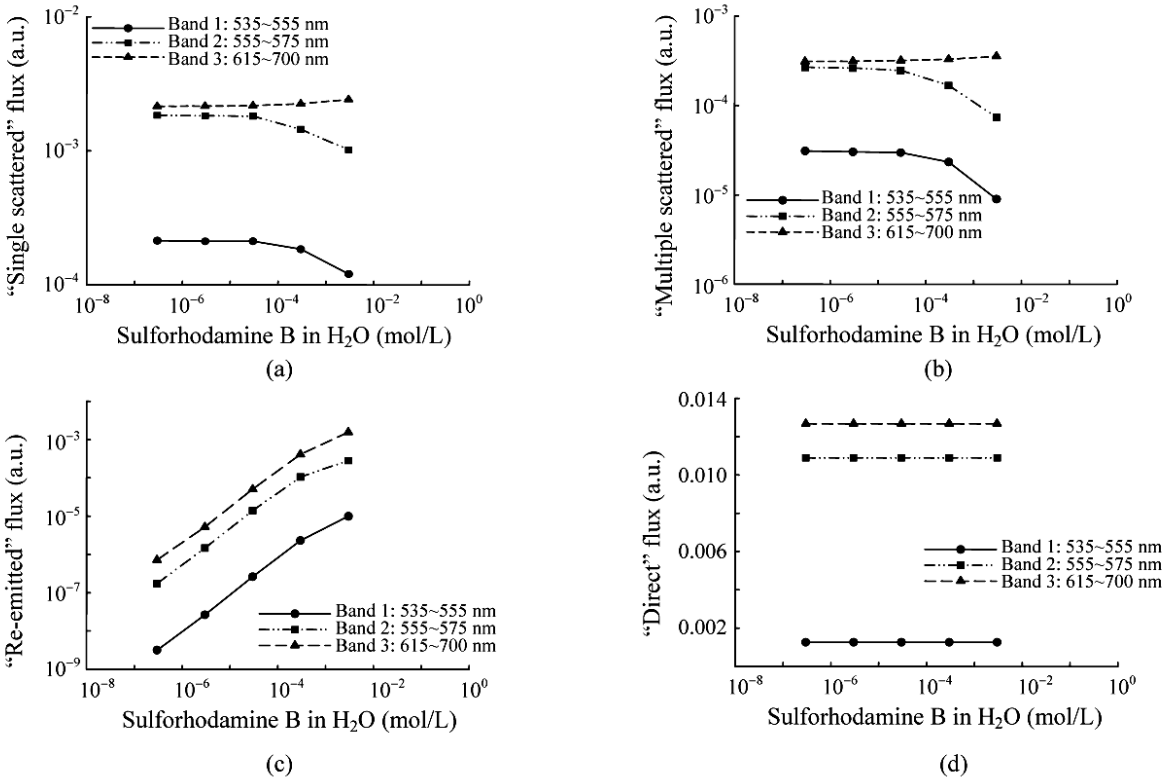

Fig.5 The partial fluxes at three spectral bands versus concentration of sulforhodamine B in water, the mean droplet radius r=20 μm, and the droplet concentration of 10^9 droplets/m^3 at 20 °C. (a) "single scattered" flux; (b) "multiple scattered" flux; (c) "re-emitted" flux; (d) "direct" flux

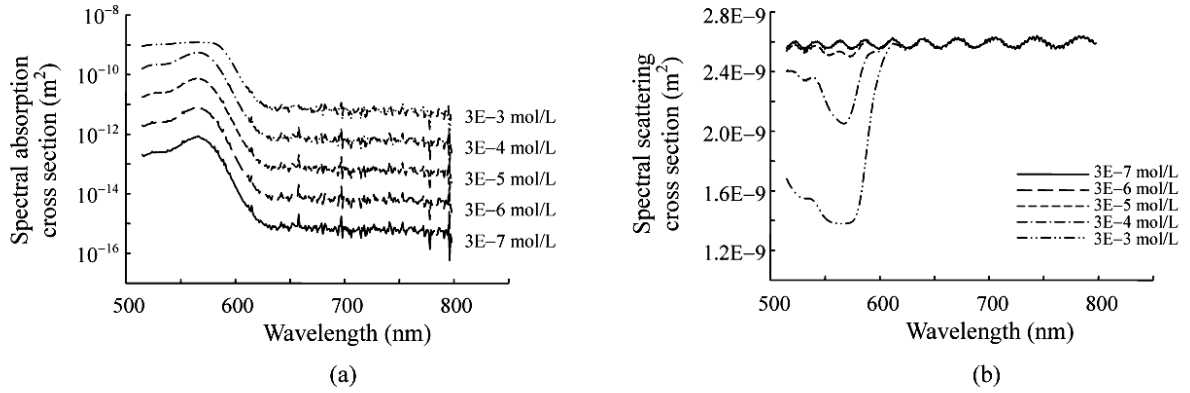

Fig.6 The cross sections of the droplet at several concentrations of sulforhodamine B in water with 10^9 droplets/m^3 at 20 °C, the mean droplet radius is 20 μm. (a) The absorption cross section $C_{abs,\lambda}$; (b) The scattering cross section $C_{sca,\lambda}$

Compared with the spectral bands 1 and 2, the value of the absorption cross sections in the band 3 is smaller by two orders of magnitude. Therefore, almost all the collision events belong to scattering ones. On Fig.5c, we observe logically that the scattering fluxes for this spectral band are not sensitive to the dye concentration.

Because the fluorescent wavelength after re-emission is larger than the incident one, the collisions of absorption followed by re-emission lead to the possibility that photons are emitted at wavelengths shorter than band 3, but re-emitted at band 3. Such re-emitted collisions may occur before single, or multiple scattering collisions events. A slight increase of the scattering fluxes for the highest dye concentrations can be observed on Fig.5a and Fig.5b, because the number of such photons increases with the dye concentration. The probability of absorption followed by re-emission is driven by the competition of absorption and scattering. Because of the increase of $C_{\mathrm{abs},\lambda}$ versus the dye concentration, as seen in Fig.6a, a large number of absorption and re-emission events occur for higher dye concentrations. The simulated results on Fig.5c verified this possibility.

The "direct" flux coming from the source "droplet" is deduced from:

$$q_{\mathrm{direct}}=W_0\exp[k_{\mathrm{ext},\lambda}(0.5D_{\mathrm{c}}+X_{\mathrm{c}})]\mathrm{d}\boldsymbol{\Omega}_s/(4\pi), \quad (16)$$

where W_0 is the initial LIF flux of the source.

On Fig.5d we observe that, for the given distance between the cylinder axis and the receptor, the "direct" flux from the source keeps unchanged with the dye concentration between 3×10^{-7} and 3×10^{-3} mol/L.

2. The effects of the concentration of droplets

On Figs.7a~7c, a similar increase of spectral fluxes is observed after collisions events for droplets concentrations lower than 10^{10} droplets/m^3. For higher droplets concentrations, increasing the concentration leads to the decrease of "single scattered" fluxes linked to the increase of multiple scattering events and fluxes. The plat in Fig.7b is due to the competition of absorption and scattering. A similar behavior is observed at each spectral band.

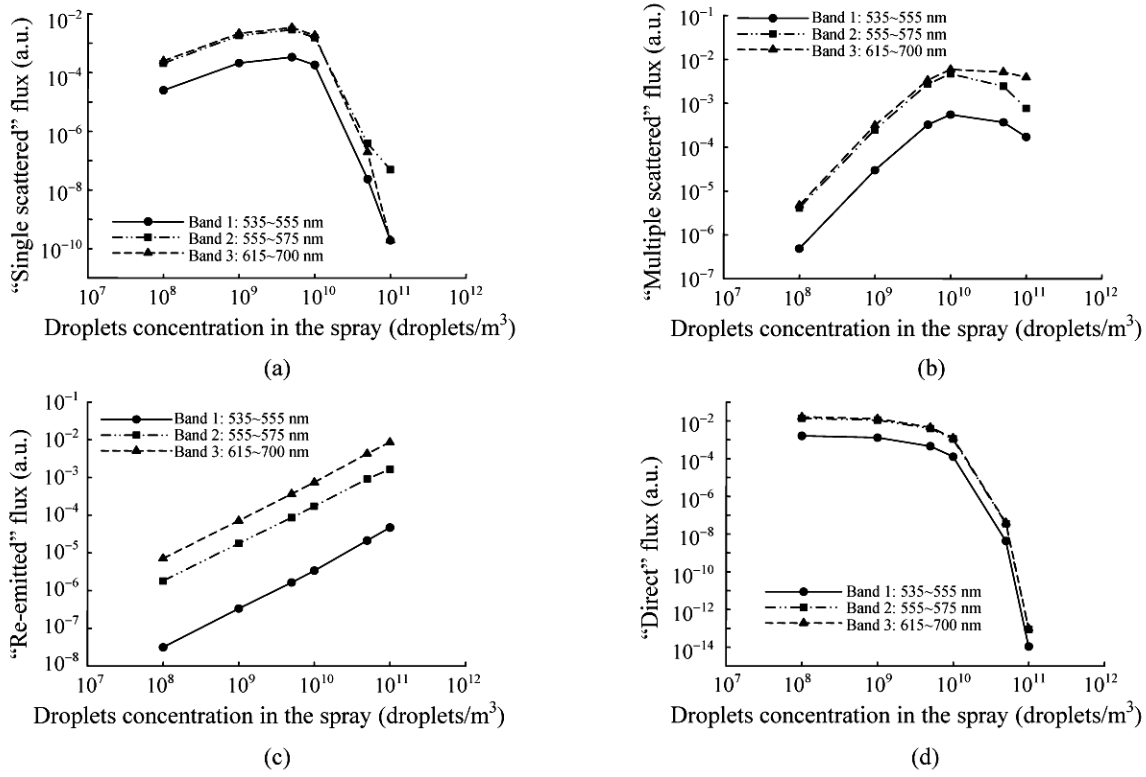

Fig.7 The partial fluxes at three spectral bands versus dyed droplets concentration. Dye concentration in water is 5×10^{-6} mol/L, and mean radius of droplets r=20 μm. (a) "single scattered" flux; (b) "multiple scattered" flux; (c) "re-emitted" flux; (d) "direct" flux

The absorption followed by a re-emission generates a logically increasing flux when the droplets concentration increases, as shown in Fig.7c. We notice that the "multiple scattered" fluxes present the same order of magnitude of absorption fluxes.

On Fig.7d the "direct" flux from the source droplet decreases exponentially with the droplets concentration. This corresponds to the decrease of the mean free path of LIF emitted photons.

3. The effects of droplets sizes

Fig.8a and Fig.8b show that the simulated scattered fluxes increase with the droplet size. Fig.8c is the "re-emitted" flux generated from the absorption and re-emission events with droplet sizes. All the partial LIF fluxes at the three spectral bands increase with the droplet size. Whereas, the "direct" flux generated from the source droplet decreases with the droplet size, shown on Fig.8d.

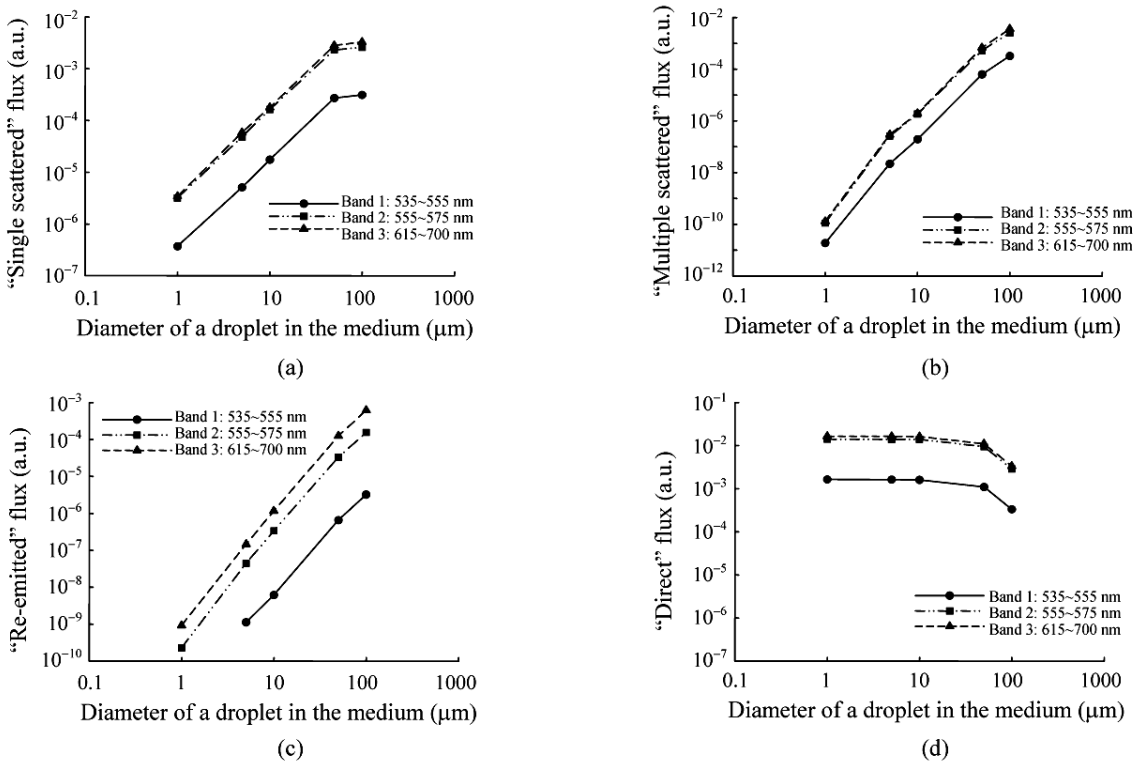

Fig.8 The partial fluxes at the three spectral bands versus droplet sizes (sulforhodamine B in water with 5×10^{-6} mol/L and 10^9 droplets/m^3 at 20 °C). (a) "single scattered" flux; (b) "multiple scattered" flux; (c) "re-emitted" flux; (d) "direct" flux

Global spectral detected LIF fluxes

The "global detected" fluxes are the total contribution from the emissive source, first, second, …, *n*th collision events. The simulated results of the spectral normalized fluxes at several droplet concentrations are shown on Fig.9.

Because the fluorescence emission occurs necessarily at a larger wavelength than the excitation one, the wavelength distribution of the resulting flux is affected by a large number of re-emission events.

When the ratio of the "re-emitted" fluxes over

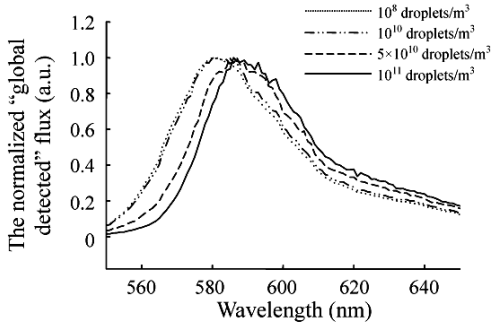

Fig.9 The normalized spectral "global detected" LIF fluxes received by the receptor versus the wavelength for several droplets concentrations

the "global detected" fluxes is significant, the number of less energetic photons increases and a "red shift" phenomenon occurs. On the figure, the computed normalized spectral LIF flux distribution exhibits such a "red shift" phenomenon with the increasing of droplets concentration in the spray.

CONCLUSION

The SMC approach was developed to predict the spectral detected LIF fluxes emitted by a polydisperse droplets spray considering the optical properties of spectrally emission, anisotropic scattering, absorption, and re-emission.

The SMC simulation performed for successive scattering, absorption and re-emission events presents the advantage of distinguishing the influences of absorption, scattering and re-emission of photons on the measurements sensitivity.

The detected LIF fluxes have been estimated at the three spectral bands representing different optical properties of liquid droplets. The computation presented here demonstrates that the detected LIF fluxes are strongly affected by the presence of droplets between the LIF control volume and the receptor. The influences of the spray parameters are not uniform along the wavelengths spectrum, but depend on the dye concentrations, droplets concentrations and sizes. Furthermore, the detected spectral LIF flux distribution demonstrates an eventual "red shift" of the initial LIF profile. The SMC approach has been tested in a simple configuration test case, and will be adapted in the future to more realistic media and geometries.

ACKNOWLEDGEMENT

The authors gratefully acknowledge the team directed by Lemoine F. at the laboratory LEMTA in Nancy for their useful advices concerning LIF measurement in liquid sprays. In addition, this study would not have been possible without the Programme Sino-Francais de Recherches Advancées (PRA E01-06: Combustion propere: aspects numériques et expérimentaux).

References

Blanca, C.M., Saloma, C., 1998. Monte Carlo analysis of two-photon fluorescence imaging through a scattering medium. *Appl. Opt.*, **37**(34):8092-8102.

Bohren, C.F., Huffman, D.R., 1983. Absorption and Scattering of Light by Small Particles. Wiley, New York, p.126-127.

Brewster, M.Q., Tien, C.L., 1982. Radiation transfer in packed fluidized beds: dependent versus independent scattering. *J. Heat Transfer*, **104**:573-579.

Castanet, G., Lavieille, P., Lemoine, F., Lebouché, M., Atthasit, A., Biscos, Y., Lavergne, G., 2002. Energetic budget on an evaporating monodisperse droplet stream using combined optical methods evaluation of the convective heat transfer. *International Journal of Heat and Mass Transfer*, **45**(25):5053-5067. [doi:10.1016/S0017-9310(02)00204-1]

Chen, L.H., 2005. Study by Numerical Simulation of Impact of Multiple Scattering on Participating Media. Ph.D Thesis, Rouen University, France.

Chen, G., Mazumder, M.M., Chang, R.K., Swindal, J.C., Acker, W.P., 1996. Laser diagnostics for droplet characterization: application of morphology dependent resonances. *Prog. Energy Combust. Sci.*, **22**(2):163-188. [doi:10.1016/0360-1285(96)00003-2]

Gomez, J.A., Thompson, W.H., 2004. Monte Carlo simulations of absorption and fluorescence spectra in ellipsoidal nanocavities. *J. Phys. Chem. B*, **108**(52):20144-20154. [doi:10.1021/jp049092v]

Gouesbet, G., Gréhan, G., 2000. Generalized Lorenz-Mie theories from past to future. *Atomic Sprays*, **10**(3-5): 277-334.

Lavieille, P., Lemoine, F., Lavergne, G., Lebouché, M., 2001. Evaporating and combustion droplet temperature measurements using two-color laser-induced fluorescence. *Exp. Fluids*, **31**(1):45-55. [doi:10.1007/s003480000257]

Lavieille, P., Delconte, A., Blondel, D., Lebouché, M., Lemoine, F., 2004. Non-intrusive temperature measurements using three-color laser-induced fluorescence. *Exp. Fluids*, **36**(5):706-716. [doi:10.1007/s00348-003-0748-0]

Lemoine, F., Antoine, Y., Wolff, M., Lebouché, M., 1999. Simultaneous temperature and 2D velocity measurements in a turbulent heated jet using combined laser-induced fluorescence and LDA. *Exp. Fluids*, **26**(4):315-323. [doi:10.1007/s003480050294]

Rozé, C., Girasole, T., Méès, L., Gréhan, G., Hespel, L., Delfour, A., 2003. Interaction between ultra short pulses and a dense scattering medium by Monte Carlo simulation: consideration of particle size effect. *Optics Communications*, **220**(4-6):237-245. [doi:10.1016/S0030-4018(03)01415-9]

Wang, L.H., Jacques, S.L., Zheng, L.Q., 1995. MCML—Monte Carlo modeling of light transport in multi-layered tissues. *Computer Methods and Programs in Biomedicine*, **47**(2):131-146. [doi:10.1016/0169-2607(95)01640-F]